

---

EFDA–JET–CP(02)07/16

J.-M. Noterdaeme, R. Budny, A. Cardinali, C. Castaldo, R. Cesario, F. Crisanti, J. de Grassie, D.A. D'Ippolito, F. Durodié, A. Ekedahl, E. Joffrin, D. Hartmann, J. Heikkinen, T. Hellsten, T. Jones, V. Kiptily, Ph. Lamalle, X. Litaudon, F. Nguyen, J. Mailloux, M. Mantsinen, M. Mayoral, D. Mazon, F. Meo, I. Monakhov, J.R. Myra, J. Paméla, V. Pericoli, O. Sauter, Y. Sarazin, S.E. Sharapov, A.A. Tuccillo, and D. Van Eester

# Heating, Current Drive and Energetic Particles Studies on JET in Preparation of ITER Operation



# Heating, Current Drive and Energetic Particles Studies on JET in Preparation of ITER Operation

J.-M. Noterdaeme<sup>1</sup>, R. Budny<sup>2</sup>, A. Cardinali<sup>3</sup>, C. Castaldo<sup>3</sup>, R. Cesario<sup>3</sup>, F. Crisanti<sup>3</sup>,  
J. de Grassie<sup>4</sup>, D.A. D'Ippolito<sup>5</sup>, F. Durodié<sup>6</sup>, A. Ekedahl<sup>7</sup>, E. Joffrin<sup>7</sup>, D. Hartmann<sup>1</sup>,  
J. Heikkinen<sup>8</sup>, T. Hellsten<sup>9,10</sup>, T. Jones<sup>11</sup>, V. Kiptily<sup>11</sup>, Ph. Lamalle<sup>4,6</sup>, X. Litaudon<sup>7</sup>,  
F. Nguyen<sup>7</sup>, J. Mailloux<sup>11</sup>, M. Mantsinen<sup>12</sup>, M. Mayoral<sup>11</sup>, D. Mazon<sup>7</sup>, F. Meo<sup>1</sup>,  
I. Monakhov<sup>11</sup>, J.R. Myra<sup>5</sup>, J. Paméla<sup>10</sup>, V. Pericoli<sup>3</sup>, O. Sauter<sup>13</sup>, Y. Sarazin<sup>7</sup>,  
S.E. Sharapov<sup>11</sup>, A.A. Tuccillo<sup>7</sup>, D. Van Eester<sup>6</sup>  
and contributors to the EFDA-JET workprogramme\*

<sup>1</sup>Max-Planck-Institut für Plasmaphysik, Euratom Association, Garching, Germany,

<sup>2</sup>PPPL Princeton, NJ, USA,

<sup>3</sup>ENEA, Euratom Association, Frascati, Italy,

<sup>4</sup>General Atomics, San Diego, CA, USA,

<sup>5</sup>Lodestar Research Corporation, Boulder, Colorado, USA,

<sup>6</sup>Association Euratom-Belgian State, LPP-ERM/KMS, Belgium,

<sup>7</sup>Association Euratom-CEA, Cadarache, France,

<sup>8</sup>Association Euratom-Tekes, VTT Processes, Finland,

<sup>9</sup>NFR, Euratom Association, Sweden,

<sup>10</sup>EFDA-CSU JET, UK,

<sup>11</sup>UKAEA, Euratom Association, UK,

<sup>12</sup>Association Euratom-Tekes, Helsinki University of Technology, Finland,

<sup>13</sup>CRPP, EPFL, Euratom Association, Lausanne, Switzerland,

“This document is intended for publication in the open literature. It is made available on the understanding that it may not be further circulated and extracts or references may not be published prior to publication of the original when applicable, or without the consent of the Publications Officer, EFDA, Culham Science Centre, Abingdon, Oxon, OX14 3DB, UK.”

“Enquiries about Copyright and reproduction should be addressed to the Publications Officer, EFDA, Culham Science Centre, Abingdon, Oxon, OX14 3DB, UK.”

## **ABSTRACT.**

This paper summarizes the recent work on JET in the three areas of heating, current drive and energetic particles. The achievements have extended the possibilities of JET, have a direct connection to ITER operation and provide new and interesting physics. Toroidal rotation profiles of plasmas heated far off axis with little or no refueling or momentum input are hollow with only small differences on whether the power deposition is located on the low field side or on the high field side. With LH current drive the magnetic shear was varied from slightly positive to negative. The improved coupling (through the use of plasma shaping and CD<sub>4</sub>) allowed up to 3.4MW of P<sub>LH</sub> in ITB plasmas with more than 15MW of combined NBI and ICRF heating. The q profile with negative magnetic shear and the ITB could be maintained for the duration of the high heating pulse (8s). Fast ions have been produced in JET with ICRF to simulate alpha particles: by using third harmonic <sup>4</sup>He heating, beam injected <sup>4</sup>He at 120 kV were accelerated to energies above 2MeV, taking advantage of the unique capability of JET to use NBI with <sup>4</sup>He and to confine MeV class ions. ICRF heating was used to replicate the dynamics of alpha heating and the control of an equivalent Q = 10 “burn” was simulated.

## **1. INTRODUCTION**

The achievements on JET of the recent years (2000-2002) [1] in the areas of heating, current drive and fast particles are directly relevant to the operation of ITER, have extended the capabilities of JET and have uncovered new and interesting physics.

The power in ITER (alpha particle heating and additional heating) will heat mainly the electrons and will not contribute significantly to plasma refueling or external momentum input. In contrast, in most present day experiments ion heating dominates and is strongly coupled with refuelling and momentum input. Some of the thus obtained results could well be inherent to this combination of properties. Experiments on JET addressed issues such as plasma rotation with heating methods/scenarios whose properties are more similar to those of the heating on ITER.

The current profile plays an important role in transport and in the stability of discharges. Advanced scenarios on ITER will require achieving and controlling the required current profiles with minimal power. Control scenarios have been developed on JET using LHCD. Other methods to drive current are being investigated.

Energetic particles will be an integral part in the operation of ITER and may dominate its behavior. Fast particles have been produced in JET using different ICRF scenarios and effects related to the presence of those fast particles have been investigated.

## **2. HEATING AND PLASMA CONTROL IN CONVENTIONAL SCENARIOS**

Rotation in present machines is often dominated by the external momentum input due to the beam heating. In ITER, the external momentum input will be strongly reduced. As rotation will remain important in several areas such as energy transport and MHD stability, we need to understand the rotation even without major external momentum input. Ion cyclotron heating in the H minority heating regime was used to investigate on JET the toroidal rotation under those conditions. Spatially resolved

rotation profiles have been obtained for the first time. A variety of experimental parameters were covered: on- and off-axis position of the resonance layer, high field side and low field side, co-, counter-, and symmetric antenna spectra, L and H mode [3- 5]. Despite the almost complete absence of external momentum input, a central co- rotation speed of up to 30 km/s is obtained with only 3MW of central power in L-mode. Far off-axis heating (Fig.1(a)), leads to centrally hollow profiles (Fig. 1(b)), with similar values for the off-axis co-rotation maximum.

With a magnetic field of 2.8T, the location of the resonance layer is moved by changing the resonance frequency (51MHz for High Field Side -HFS- resulting in  $R_{\text{res}} = 2.53\text{m}$ , and 37MHz for Low Field Side -LFS- resulting in  $R_{\text{res}} = 3.49\text{m}$ ). The central electron temperature is 3keV, the central plasma density  $3 \times 10^{19} \text{m}^{-3}$ . In contrast to predictions of theories that rely on fast particle effects to produce the rotation, there is no significant difference in the rotation profile between a high field side and a low field side position of the resonance layer (Fig. 1(b)). This points, for those conditions of far off-axis heating to other mechanisms than fast particles as the reason for these rotation profiles. A check of this hypothesis will be made on JET using pure electron off-axis heating through ICRF mode conversion heating.

The dependence of the shape of the rotation profile on the distance of the resonance layer from the center can be clearly seen when the resonance layer is moved by changing the magnetic field at constant frequency: the hollow profile becomes peaked. When however the resonance is central and leads to a stabilization and a subsequent crash of the sawteeth, the appearance of MHD modes can lead to a breaking of the rotation and a very flat rotation profile [5, 6]. The difference between L ( $P_{\text{ICRH}} = 2\text{MW}$ ) and H-mode ( $P_{\text{ICRH}} = 9\text{MW}$ ) is shown in Fig.1(c) for a slightly off-axis position of the resonance layer ( $R=2.70\text{m}$ ).

ICRF mode conversion heating ( $^3\text{He}$  in D and  $^4\text{He}$ ) has been further developed on JET [7] and can now be used as a localized on- or off-axis source of electron heating for, among others, rotation experiments without external momentum input and fast particle effects and for electron transport studies. By proper programming of the  $^3\text{He}$  gas flow, a steady state off-axis peaked power deposition on the electrons was maintained throughout the ICRF heating phase (up to 5s, limited only by technical constraints). Figure 2 shows time traces for this experiment, the profile measured by modulation techniques, and for comparison the theoretical calculations obtained for a single  $N_{\parallel}$  from the full wave code ALCYON, combined with ray tracing (to follow the deposition of the short wavelength mode converted ion Bernstein wave).

The width of the profile is affected by the launched spectrum: the  $-90^\circ$  phasing, leading to a wave propagating in the counter- current direction (the current is clockwise and co-linear with B), results in a more peaked profile.

In ITER, because of the strong central heating and, in addition, the large central pressure of fast particles, it may be necessary to control the sawteeth to avoid too large central temperature and power excursions. The gradient of the current profile at the  $q = 1$  surface and the fast particle pressure inside the  $q = 1$  surface affects the stability of sawteeth. Both can be modified with the ICRF minority scenario using an asymmetric antenna spectrum. Monster (stabilized) sawteeth and very small

(destabilized) sawteeth can thus be produced. Asymmetric spectra at the fundamental and second harmonic [8-10] of H have been used. Figure 3 shows time traces of an experiment where fundamental heating of H (10% concentration) in a D plasma was used. The H cyclotron resonance layer was located on the high field side (HFS) and the toroidal magnetic field was ramped up ( $B_T = 2.3 \rightarrow 2.8$  T). Sawteeth stabilization was observed with  $+90^\circ$  phasing, corresponding to waves directed along the plasma current. With  $-90^\circ$  phasing, the sawteeth had a shorter period. However, even with this phasing, monster sawteeth appeared at a higher field. Both a change of the shear profile due to the minority CD [11, 12] localized around the  $q = 1$  surface as well as fast particle pressure effects [13] must be invoked to explain the observed results. The latter are enhanced in the case of  $+90^\circ$  phasing by an ICRF induced pinch in the presence of directed waves [14, 15], see section 3, leading to more fast particles inside the  $q = 1$  surface. Small sawtooth periods (obtained with  $-90^\circ$  phasing) avoid the appearance of NTMs which otherwise grow after a sufficiently large seed island is created at the crash of a sawtooth with a long period [16].

The experiments above show that it may be desirable to couple ICRF power with a variety of phasing between current straps to encompass both heating and current drive/control applications. One may even want to use different phasings on different antennas at the same time (“mixed-phasings”) for simultaneous optimization of core and edge plasmas [17, 18]. One of the limiting factors in using phasings other than those resulting in a symmetric spectrum with no power at  $k_{\parallel} = 0$  (e.g. so called dipole phasing) is the occurrence of RF sheath interactions at the antenna. This can have negative consequences such as a reduced heating efficiency, hot spots and arcs, and impurity production. However, the use of phasings with substantial power in the  $k_{\parallel} = 0$  component of the spectrum (e.g. monopole phasing) can also have some beneficial properties through RF-driven edge convection: it can affect the particle confinement time and the repetition rate of the ELMs (Edge Localized Mode), and reduce the divertor heat load by broadening the SOL. Recent mixed-phasing experiments on JET thus explored the combination of antennas in dipole phasing to heat the central plasma with antennas in monopole phasing to control the edge by locally increasing the transport. In L-mode, unexpected strong deleterious interactions between adjacent monopole and dipole antennas were observed, which did not occur when all the antennas were in either monopole or dipole [18]. The interactions were attributed to arcing caused by sheath-driven currents, where the currents are driven by asymmetric sheath potentials on the two antennas and propagate via sheath-induced radial convection of the current [18]. Calculations suggest that the mixed-phasing approach may be more successful for H-mode plasmas because the local density near the antenna (and thus the sheath currents) are smaller in H-mode. This idea will be tested in future campaigns.

### **3. CURRENT AND PRESSURE PROFILE CONTROL IN PLASMAS WITH STRONG INTERNAL TRANSPORT BARRIERS**

Lower hybrid co-current drive and heating was used to vary the shape of the  $q$  profile, more specifically the magnetic shear from slightly positive to negative. With negative shear, strong internal transport barriers could be obtained at much lower power than previously, widening the parameter space in which strong ITB could be explored. The coupling of the LH wave in H-mode plasmas

was greatly improved by puffing  $CD_4$  near the launcher and matching the plasma shape [19, 20]. As a result, up to 3.4MW of  $P_{LH}$  was coupled in ITB plasmas with more than 15MW of NBI and ICRF heating. This possibility to combine LH with strong additional power has allowed for the first time in JET, real-time control of ITB discharges for the duration of the heating pulse (up to 7.5s) [21, 22, 23]. Quasi-stationary operation has thus been achieved in high performance discharges with a large bootstrap fraction. A simple criterion was used to characterize the ITB existence, its location and strength [24]. Simultaneous real-time feedback control on the electron temperature gradient (with ICRH) and the neutron yield (with NBI) (Fig.4) [21, 22] has allowed to reach quasi-steady state in a more reproducible way. Disruption core collapses and impurity accumulation could be mitigated while the ITB regime was sustained. One of the main conclusions from those experiments was that the LHCD, which was not feedback controlled, froze the current profile and so the ITB position [25].

Subsequently, attempts were made to control also the current density profile. A simple case was chosen to demonstrate the feasibility of applying a ‘model based control’. During an extended preheat LHCD phase at low density ( $2.7 \times 10^{19} \text{ m}^{-2}$ ), the objective was to reach a predefined q-profile in conditions where all the others parameters were maintained constant. The plasma current was fixed at 1.5MA and  $B_T = 3T$ . The feedback control on the current profile was applied on 5 point located at 5 fixed normalized radii. The target was reached perfectly and a comparison with a non-controlled shot shows the efficiency of the control in preventing monotonic relaxation. In that discharge 40% of the total current was ohmically driven.

A new IBW power coupling scheme by Mode Conversion of 5MW externally launched Fast Wave power has been successfully tested in a D-3He plasma of the JET tokamak. The damping of the MC wave was on the Deuterium ions and this induced near the edge a poloidal sheared flow with  $E \times B$  shearing rate of 5MHz, much higher than the threshold for turbulence suppression. In the same region, a large ( $R_{ITB} \sim 3.75m$ ), stationary ITB was indeed formed, and the plasma pressure increased in the overall plasma volume [26, 27].

Fast wave current drive on ITB and mode conversion current drive are also being tested in JET on their suitability as control tools [28]. Some ICRF power (2-3 MW) has been coupled in a FWCD scenario first in L-mode at high toroidal magnetic field ( $B_0 = 3.45 \text{ T}$ ,  $f_{ICRF} = 37 \text{ MHz}$ ,  $I_p = 2.5 \text{ MA}$ ) [29] without strong parasitic ion cyclotron absorption. The central electron temperature is 4 keV. The current density profiles at the center between  $+90^\circ$  (Pulse No: 51643) and  $-90^\circ$  (Pulse No: 51644) phasings (Fig.5) deduced from Motional Stark Effect measurements are clearly different. This is to be compared with current drive simulations performed with the ALCYON and TORIC codes that gives 30kA per MW of ICRF power coupled to plasma in this configuration. With 2MW of LH preheating and with an additional 4.2MW of ICRF power in the main heating phase, a central electron temperature of 6keV has been achieved in this FWEH scenario. Furthermore, when 7.5MW of NBI and 6MW of ICRH were applied in the main heating phase of this scenario, an electron ITB was obtained with a central electron temperature of 8 keV. This type of advanced scenario is thus promising for current profile control on JET as the single pass absorption on the electrons and the current drive efficiency increase strongly with electron temperature.



#### 4. BURNING PLASMA SIMULATIONS AND ENERGETIC PARTICLE ISSUES

The dynamics of alpha particle heating and control of an equivalent  $Q = 10$  burn was experimentally investigated by using H minority heating. Part of the heating was employed to simulate the alpha heating  $P_{\alpha, \text{sim}}$ , as calculated in real time from the measured plasma parameters and the other part  $P_{\text{aux}}$  was used to control this “burn”. Two alternative algorithms were adopted for the real-time computation of  $P_{\alpha, \text{sim}}$  the simulated alpha power. The experiments were performed in the ELMy H-mode in a divertor configuration with  $q_{05} \approx 3$ . A qualitatively similar trajectory of the discharge was programmed as that foreseen for a reactor in terms of  $P_{\text{aux}}$  and density ramp-up. The magnetic field, power level and density were therefore all chosen to ensure that the L-H transition occurred towards the end of the  $P_{\text{aux}}$  ramp. It was possible to meet these requirements, assuming a maximum of 10MW ICRH was available, at 2.5MA/2.5T. The first algorithm to calculate the simulated alpha power was based on the measured  $R_{\text{DD}}$  rate: when ICRH is superposed onto a baseline level of 2MW NBI, the observed change of DD reaction rate ( $\Delta R_{\text{DD}}$ ) varies as  $T_e(0)^{1.5-2.0}$ , i.e. similar to the approximate scaling of R DT in the reactor-relevant temperature range. Therefore, in the first experiments we used  $P_{\alpha, \text{sim}}(t) = C_{\alpha} \cdot \Delta R_{\text{DD}}(t)$ . In the second series of experiments, the algorithm for  $P_{\alpha, \text{sim}}(t)$  was based on a parametrised fit to the volume-integral of thermal DT reaction rate  $R_{\text{DT}}$  (for 50:50 D:T mix) in terms of  $T_e(0)$ , and volume average  $\langle T_e \rangle$ ,  $\langle n_e \rangle$ , assuming  $T_e = T_i$  and flat  $n_e(r)$  profile i.e.

$$P_{\alpha, \text{sim}}(t) = C_{\alpha} \cdot R_{\text{DT, sim}}(t) = C_{\alpha} \cdot n_e(0)^2 \cdot F(S_T \cdot T_e(0), T_e(0)/\langle T_e \rangle)$$

where  $S_T = T_{\text{reactor}}/T_{\text{JET}} \approx 3$  and  $F$  is the parametrised fit function. In both algorithms,  $C_{\alpha}$  was chosen to obtain  $Q_{\text{eff}} = 5P_{\alpha, \text{sim}}/P_{\text{aux}} \approx 10$  at maximum ICRH power.

From simple power balance considerations, a number of distinct operating regimes may be identified, depending on the value of  $Q_{\text{eff}}$ . For  $0 < Q_{\text{eff}} < Q_{\text{runaway}}$  the system is unconditionally stable. For  $Q_{\text{eff}} > Q_{\text{runaway}}$ , a change of plasma thermal energy  $W$  results in a change of  $P_{\alpha, \text{sim}}$  greater than the increase of the loss power ( $P_{\text{loss}}$ ) arising through transport mechanisms. In this second regime, the simulated alpha power is expected to be subject to an unstable excursion but  $P_{\text{aux}}$  can be reduced to compensate, thus feedback control of the alpha power via  $P_{\text{aux}}$  should be possible. In a fully ignited plasma the alpha power exceeds  $P_{\text{loss}}$ , so some burn control mechanism other than  $P_{\text{aux}}$  would then be required. One of the main aims of the present experiments was to demonstrate the qualitative features of the onset of “thermal runaway” in the unstable finite  $Q_{\text{eff}}$  regime ( $Q_{\text{eff}} > Q_{\text{runaway}}$ ), and then to stabilize the runaway using feedback control of  $P_{\text{aux}}$ . Results obtained in the first scenario [ $P_{\alpha, \text{sim}}(t) \propto \Delta R_{\text{DD}}(t)$ ] are presented in Fig.6, showing the evidence of onset of thermal runaway for  $Q_{\text{eff}} \approx 8$ . Note also the strong variation in  $P_{\alpha, \text{sim}}$  due to sawteeth, and the partially compensating effect of  $P_{\text{aux}}$ . At  $t = 20$ s a combination of feedforward and feedback control of the  $P_{\text{aux}}$  component of the ICRF power was used to stabilize  $P_{\alpha, \text{sim}}$  at a reference level which was stepped up as shown during the steady-state controlled phase in order to observe the overall system response. The gain  $G$  of the feedback loop was set to  $G \approx (P_{\alpha, \text{sim}}/P_{\text{aux}}) = Q_{\text{eff}}/5 \approx 3$ , and an integral term  $f \approx (1/\tau E)$  was used.

The second scenario [ $P_{\alpha,\text{sim}}(t) \propto R_{\text{DT},\text{sim}}(t)$ ], produces similar features as the first scenario, except that the thermal instability is more pronounced, reflecting the more realistic density and temperature dependence of  $P_{\alpha,\text{sim}}$ . The  $P_{\text{aux}}$  component of the heating was controlled under feedback, using similar feedback loop parameters as in the first scenario, and the excursion in  $P_{\alpha,\text{sim}}$  was still satisfactorily stabilized.

It should be noted that there are fundamental limitations to these kinds of scale-model experiments of reactor-like scenarios, e.g. it is not possible to preserve all the relevant dimensionless timescales such as the ratio of thermal energy confinement time to fast-ion slowing-down time  $\tau_s/\tau_E$ . This discrepancy will affect the dynamic behavior; it is in fact not possible to satisfy all the required similarity conditions simultaneously, and this ultimately limits the fidelity of the experimental simulations. Nevertheless, several of the expected dynamic features of self-heated plasmas have been demonstrated in the present work.

Experiments have been carried out for the first time on JET with the 3<sup>rd</sup> harmonic ion cyclotron resonance heating of  $^4\text{He}$  beam ions in order to produce a high-energy population of  $^4\text{He}$  ions to simulate 3.5MeV fusion-born alpha particles [30]. Up to 8MW of ICRH power was applied at a frequency of 51MHz at a magnetic field of 2.2T, placing the 3<sup>rd</sup> harmonic  $^4\text{He}$  ion cyclotron resonance,  $\omega \approx 3c(^4\text{He})$ , in the plasma center. In order to ensure significant 3<sup>rd</sup> harmonic absorption strength,  $^4\text{He}$  neutral beam ions with energy in the range of 70-120keV were added (Fig.7). The successful acceleration of  $^4\text{He}$  beam ions to the MeV energy range by the ICRH was confirmed by measurements of gamma ray emission from the reaction  $^9\text{Be}(\beta, n)^{12}\text{C}$  [31] and excitation of Alfvén eigenmodes [32, 33], and was consistent with the observed heating of the background electrons and sawtooth stabilization. The largest high-energy populations of the alpha particles were obtained with the highest energy  $^4\text{He}$  beams, as expected. This scheme will be used in the forthcoming JET campaign with  $^4\text{He}$  plasmas for dedicated alpha-particle studies, such as for study of parasitic absorption of lower hybrid power by alpha particles.

Direct evidence for the wave-induced pinch of fast ions in the presence of asymmetric ICRF waves (co-current spectrum leading to an inward pinch and a counter-current spectrum to an outward pinch) was obtained [34]. This was made possible by recent advances in the tomographic reconstruction of the measured  $\gamma$ -ray emission data [31]. With waves launched predominantly in the co-current direction, a higher radial gradient of  $\gamma$ -ray emission, and thus of fast ions, was obtained than with waves in the counter-current direction. This result together with concurrent differences in Alfvén eigenmodes, sawtooth periods, electron temperatures and fast ion energies show that the ICRF-induced pinch can provide a tool to affect the radial fast ion profile and the plasma heating profile during ICRF.

## 5. PROSPECTS

We plan to make further progress in the coupling of LH power to ITER relevant edge conditions. Advances in the coupling of more ICRF power in type I ELMy H-modes, which will be of substantial benefit to the experimental program, follows a double approach. On the short time scale, electronic

measures are being implemented to improve the reaction of the generator protection system to the effects of repeated ELMs. On a slightly longer time scale, an ITER-like ICRF antenna, which incorporates several ELM resilient features such as conjugate matching and 3 dB couplers will be installed. This new antenna and the installation of 3 dB couplers on two of the existing ICRF antennas are expected to increase the ICRF power available on discharges with strong type I ELMs to 12MW or more.

## REFERENCES

- [1]. TUCCILLO A.A., BARANOV Y. et al., “Recent Heating and Current Drive Results on JET”, Radio Frequency Power in Plasmas, (14th Topical Conf., Oxnard, CA, 2001), Vol. 595, AIP (2001) 209-216.
- [2]. BUDNY R.V., CHANG C.S. et al., “Comparison of theory of ICRH-induced torques with rotation measurements in JET plasmas”, Contr. Fusion and Plasma Phys., (28th EPS Conf., Funchal (Madeira), Portugal, 2001), Vol. ECA 25A, EPS (2001) 481-484.
- [3]. NOTERDAEME J.-M., RIGHI E. et al., “Spatially resolved plasma rotation profiles with ICRF on JET”, Radio Frequency Power in Plasmas, (14th Topical Conf., Oxnard, CA, 2001), Vol. 595, AIP (2001) 98-101.
- [4]. NOTERDAEME J.-M., RIGHI E. et al., “Toroidal plasma rotation with ICRF on JET”, Controlled Fusion and Plasma Physics, (28th EPS Conf., Funchal (Madeira), Portugal, 2001), Vol. ECA 25A, EPS (2001) 777-780.
- [5]. NOTERDAEME J.-M., RIGHI E. et al., “Spatially resolved plasma rotation profiles with ICRF on JET”, subm. to Nucl. Fusion (2002)
- [6]. LAZZARO E., HENDER T.C. et al., “Anomalous braking and shear modification of plasma rotation in a tokamak”, Plasma Physics and Controlled Fusion, (29th EPS Conference, Montreux (CH), 2002), EPS (2002)
- [7]. MANTSINEN M., MAYORAL M.-L. et al., “ICRF Mode Conversion Experiments on JET”, Controlled Fusion and Plasma Physics, (28th EPS Conf., Funchal (Madeira), Portugal, 2001), Vol. ECA 25A, EPS (2001) 1745-1748.
- [8]. MANTSINEN M., MAYORAL M.-L. et al., “Analysis of ion cyclotron current drive at  $\omega = 2 \omega_{cH}$  for sawtooth control in JET plasmas”, Controlled Fusion and Plasma Physics, (28th EPS Conf., Funchal (Madeira), Portugal, 2001), Vol. ECA 25A, EPS (2001) 789-792.
- [9]. MANTSINEN M., ANGIONI C. et al., “Analysis of ion cyclotron heating and current drive at  $\omega = 2 \omega_{cH}$  for sawtooth control in JET plasmas”, accepted for publication in Plasma Phys. and Contr. Fusion (2002)
- [10]. MAYORAL M.-L., WESTERHOF E. et al., “Neo-classical Tearing mode control through sawtooth destabilisation in JET”, Controlled Fusion and Plasma Physics, (29th EPS Conference, Montreux (CH), 2002), EPS (2002)
- [11]. START D.F.H., BHATNAGAR V.P. et al., “Observation of Fast Wave Ion Current Drive Effects on Sawteeth in JET”, Controlled Fusion and Plasma Physics, (19th EPs, Innsbruck, 1992), Vol. 16 C, EPS (1992) 897-904.

- [12]. BHATNAGAR V.P., START D.H.F. et al., “Local Magnetic Shear Control in a Tokamak via fast wave minority current drive : theory and experiments in JET”, Nucl. Fus. **34** (1994) 1579-1603.
- [13]. PORCELLI F., “Fast Particle Stabilisation”, Plasma Phys. Contr. Fusion **33** (1991) 1601-1620.
- [14]. ERIKSSON L.-G., MANTSINEN M. et al., “Evidence for a Wave-Induced Particle Pinch in the Presence of Toroidally Asymmetric ICRF Waves”, Physical Review Letters **81** (1998) 1231-1234.
- [15]. JOHNSON T., HELLSTEN T. et al., “Experimental Evidence for RF-Induced Transport of Resonant He<sup>3</sup>-Ions in JET”, Energetic Particles in Magnetic Confinement Systems, (7th IAEA TCM, Gothenburg, 2001), IAEA
- [16]. SAUTER O., WESTERHOF E. et al., “Control of Neoclassical Tearing Modes by Sawtooth Control”, Phys. Rev. Letters **88** (2002) 105001.
- [17]. D’IPPOLITO D.A., MYRA J.R. et al., “Modeling of Mixed-Phasing Antenna-Plasma Interactions Applied to JET A2 Antennas”, RF Power in Plasmas, (14th Top. Conf., Oxnard, CA, 2001), Vol. 595, AIP (2001) 114
- [18]. D’IPPOLITO D.A., MYRA J.R. et al., “Modeling of mixed-phasing antenna-plasma interactions on JET A2 antennas”, accepted for publication in Nucl. Fus. (2002)
- [19]. PERICOLI V., PODDA S. et al., “LHCD coupling during H-mode and ITB in JET plasmas”, Radio Frequency Power in Plasmas, (14th Topical Conf., Oxnard, CA, 2001), Vol. 595, AIP (2001) 245-248.
- [20]. PERICOLI V., EKEDAHL A. et al., “Study and optimisation of lower hybrid waves coupling in advanced scenarios plasmas in JET”, submitted to Physics of Plasmas (2002)
- [21]. CRISANTI F., LITAUDON X. et al., “JET steady state ITB operation with active control of the pressure profile”, Physical Review Letters **88** (2002) 145004-1 -145004-4.
- [22]. MAZON D., LITAUDON X. et al., “Real-time control of internal transport barriers in JET”, Plasma Phys. Control. Fusion **44** (2002) 1087-1104.
- [23]. LITAUDON X., BÉCOULET A. et al., “Progress towards Steady -State Operation and Real Time Control of Internal Transport Barriers in JET”, Fusion Energy, (19th IAEA Conference, Lyon, 2002), EX/C3-4, this conference.
- [24]. TRESSET G., LITAUDON X. et al., “A dimensionless criterion for characterizing internal transport barriers in JET”, Nucl. Fusion **42** (2002) 520-526.
- [25]. CASTALDO C., CESARIO R. et al., “Effect of low magnetic shear induced by lower hybrid current drive on high performance internal transport barriers in JET”, Physics of Plasmas **9** (2002) 3205-3208.
- [26]. CASTALDO C., CESARIO R. et al., “Transport barriers produced in JET discharges by ion Bernstein waves”, Fusion Energy, (19th IAEA Conference, Lyon, 2002), subm., post-deadline paper, this conference.

- [27]. CARDINALI A., CASTALDO C. et al., “Modelling of ion Bernstein waves obtained by mode conversion of fast waves for local generation of plasma sheared flows”, Theory of Fusion Plasmas, (Joint Varenna-Lausanne International Workshop, Varenna, 2002), in print
- [28]. MEO F., BRAMBILLA M. et al., “Comparison of FWCD Scenarios on ASDEX-Upgrade, JET, and DIII-D Tokamaks”, RF Power in Plasmas, (14th Topical Conf., Oxnard, CA, 2001), Vol. 595, AIP (2001) 194-197.
- [29]. NGUYEN F., NOTERDAEME J.-M. et al., “ICRF Current Drive Experiments on JET”, Controlled Fusion and Plasma Physics, (28th EPS Conf., Funchal (Madeira), Portugal, 2001), Vol. ECA 25A, EPS (2001) 781-784.
- [30]. MANTSINEN M., MAYORAL M.-L. et al., “Alpha Tail Production with Ion Cyclotron Resonance Heating of He4 Beam Ions in JET Plasmas”, Phys. Rev. Letters **88** (2002) 105002-1-105002-4.
- [31]. KIPTILY V.G., CECIL F.E. et al., “ $\gamma$ -ray diagnostics of energetic ions in JET”, Nucl.Fusion **42** (2002) 999.
- [32]. JAUN A., “Collective modes and Fast Particle Confinement in ITER”, Fusion Energy, (Lyon, 2002) this conf.
- [33]. TESTA D., FASOLI A. et al., “Experimental Study of the Stability of alfvén Eigenmodes on JET”, Fusion Energy, (19th IAEA Conference, Lyon, 2002), IAEA (2002) this conference.
- [34]. MANTSINEN M., INGESSON L.C. et al., “Controlling the profile of ion-cyclotron-resonant ions in JET with the wave-induced pinch effect”, Phys. Rev. Letters **89** (2002) 115004-1-115004-4.

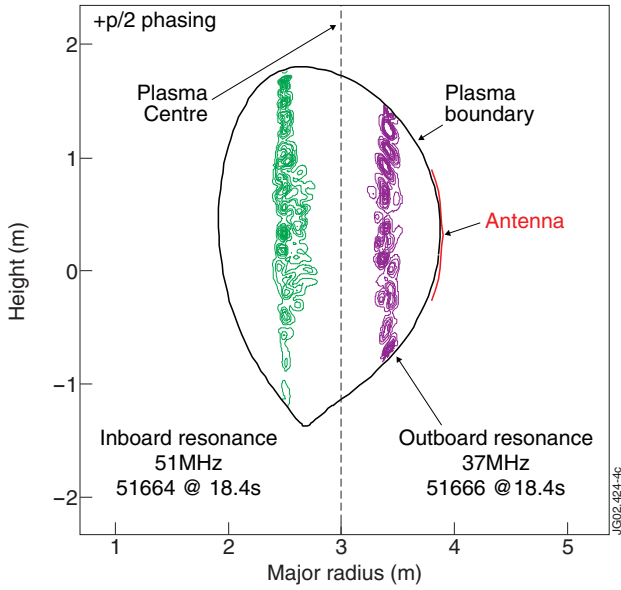


Figure 1: (a) Location of the power deposition for the resonance layer positioned at the high field side and at the low field side, calculated [2] using the SPRUCE module in TRANSP.

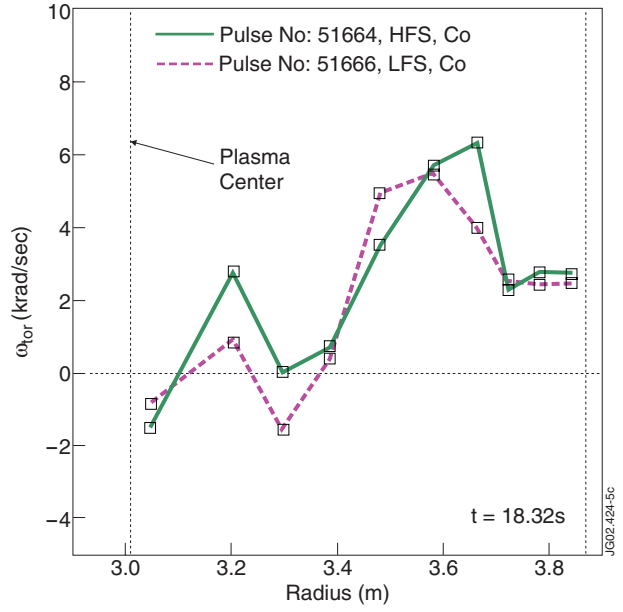


Figure 1: (b) Rotation profile, for a HFS and a LFS position of the resonance layer for a co-directed spectrum. The ICRF power is 2MW.

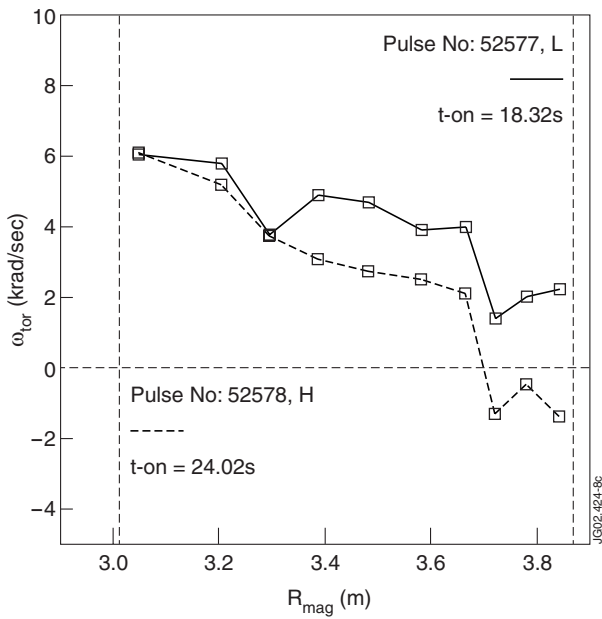


Figure 1: (c) Rotation profile, for a plasma in L and H mode for a HFS position of the layer ( $R=2.7m$ ) and a counter-directed spectrum.

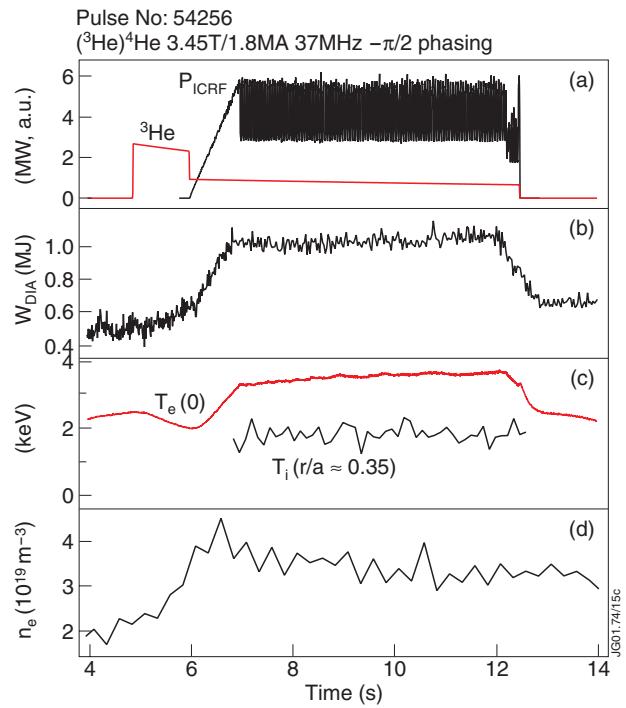


Figure 2: (a) Time traces of a discharge with  $^3\text{He}$  in  $^4\text{He}$  mode conversion scenario. ICRF power and  $^3\text{He}$  gasflow, diamagnetic energy, temperatures, averaged density.

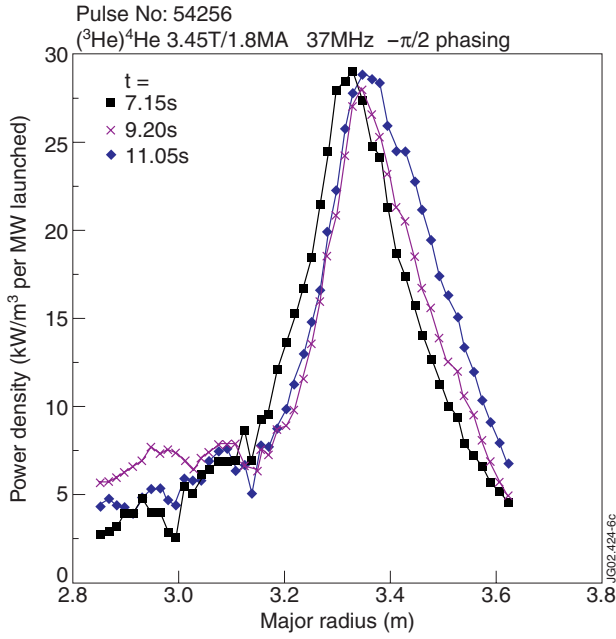


Figure 2: (b) Measured power density to the electrons based on break-in-slope analysis

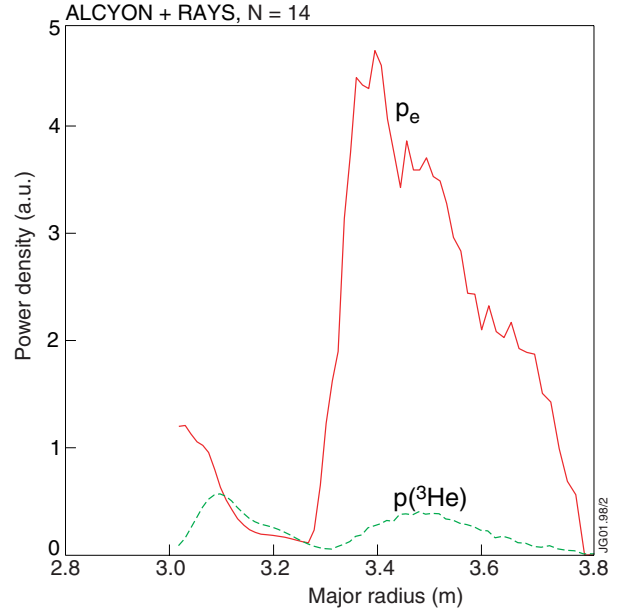


Figure 2: (c) Calculated power density to electrons and ions based on the theoretical calculations (see text).

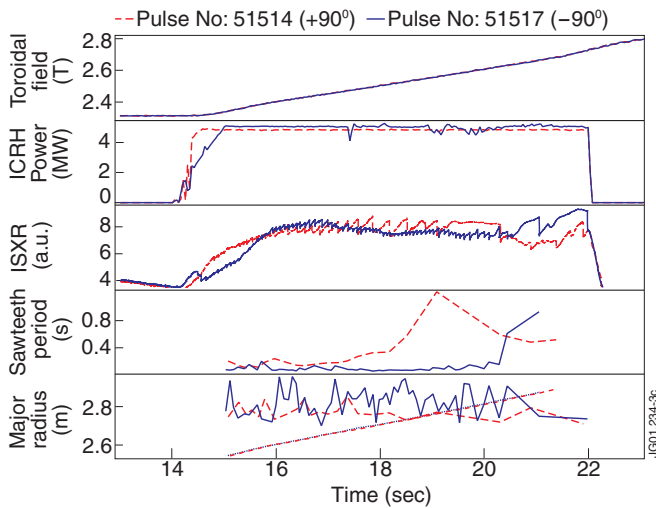


Figure 3: Time signals of two pulses with different ICRF phasing :  $+90^\circ$  (Pulse No: 51514) in red continuous line and  $-90^\circ$  (Pulse No: 51517) in blue dashed line: magnetic field ramp up, ICRF power, soft X-ray, sawteeth period, the major radius location of the ion cyclotron resonance layer (monotonically increasing) and inversion radius

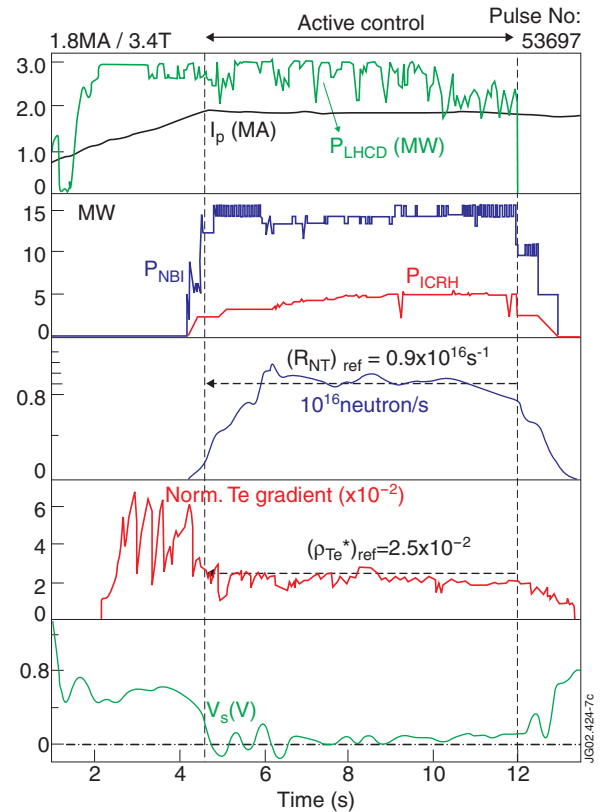


Figure 4: Control of an ITB using feedback on NBI and ICRH to control neutron rate and electron temperature gradient

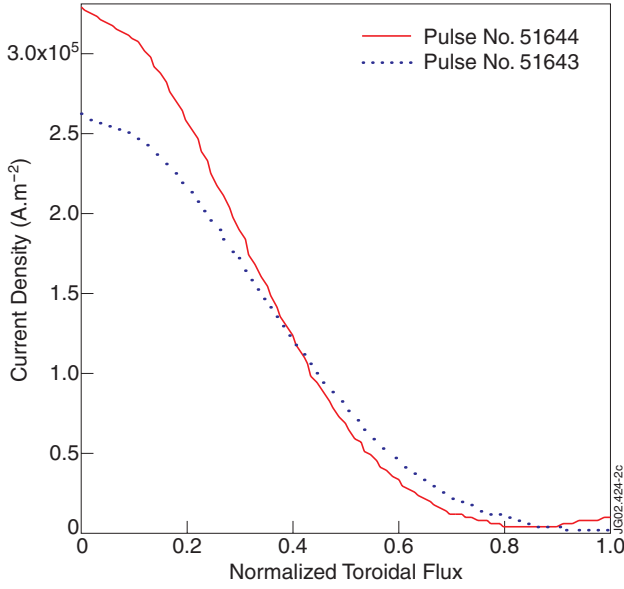


Figure 5: Current density profiles for Pulse No:51643 (+90°) and Pulse No: 51644 (-90°)

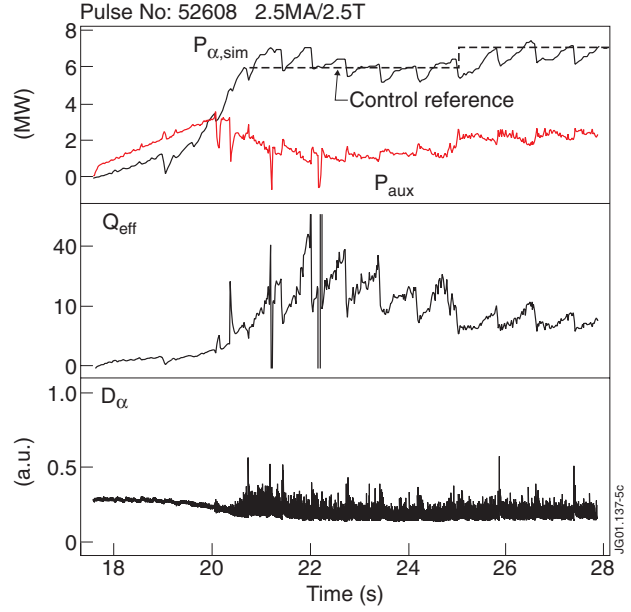


Figure 6: Step-change increase in  $P_{\alpha,sim}$  demand achieved via feedback control on  $P_{aux}$

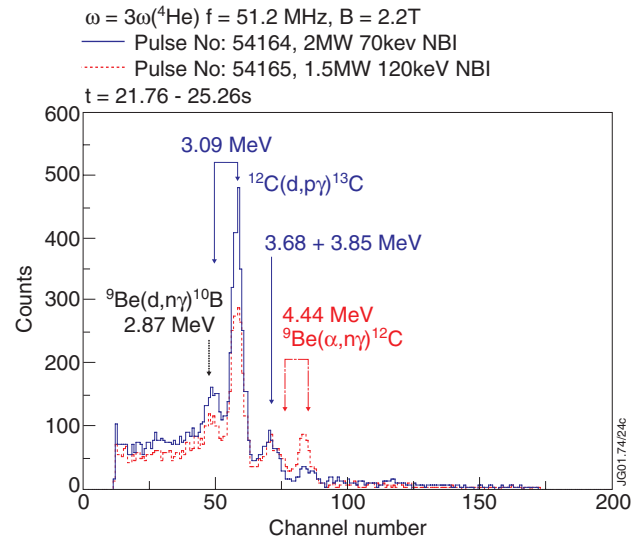
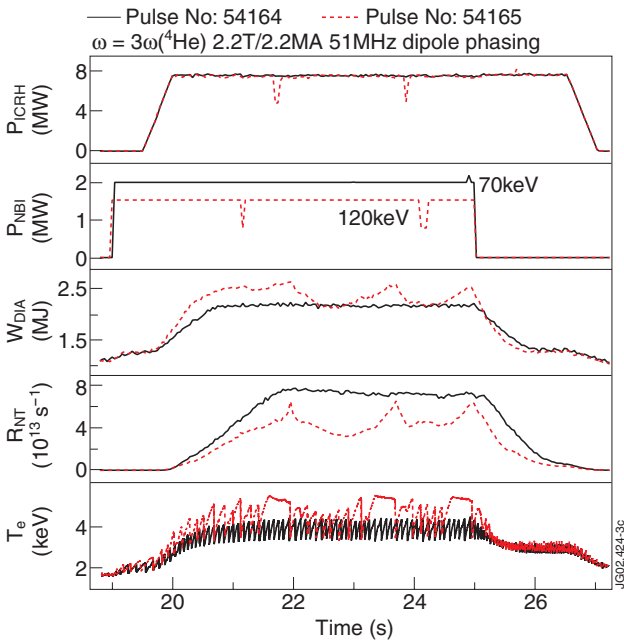


Figure 7: (left) Overview of Pulse No's: 54164 and 54165 with  $3\omega_c^4He$  heating and 70keV and 120keV  $^4He$  beams, respectively. (right) Gamma ray spectra for the same two discharges.